Quantum theory of transient transport in semiconductors: A Monte Carlo approach

(Article begins on next page)

25 August 2022

Quantum theory of transient transport in semiconductors: A Monte Carlo approach

R. Brunetti, C. Jacoboni, and F. Rossi

Dipartimento di Fisica dell'Università, Via Campi 213/A, 41100 Modena, Italy

(Received 28 November 1988)

A new Monte Carlo method is presented for the evaluation of the density matrix from the solution of the Liouville–von Neumann equation for an ensemble of noninteracting electrons in a semiconductor crystal. The method is applied to the study of the electron transient response to a high external electric field in Si and to the relaxation of photoexcited electrons in GaAs in absence of external electric fields. The phonon population is always assumed at equilibrium, but no assumptions are made about the strength of the electron-phonon interaction. Results show that typical quantum features such as energy-nonconserving transitions, intracollisional field effect, and multiple collisions change the very first transient of the system with respect to a semiclassical description.

I. INTRODUCTION

The Monte Carlo method[1] applied to the analysis of charge transport in semiconductors[2] has for almost 20 years allowed the investigation of the transport properties of a large variety of physical systems. Once the band structure and the scattering mechanisms of the material under investigation are known, this numerical technique permits a direct simulation of the behavior of the electron gas in the presence of scattering agents such as phonons and impurities. In recent years the method has also been successfully applied to problems of device design and performance that would not be otherwise attainable with traditional numerical or analytical techniques.

However, the very fast evolution of miniaturization semiconductor technology[3] is leading very rapidly towards experimental conditions where typical lengths are of the order of the carrier coherence length, and typical times are comparable with carrier relaxation times.[4] In particular, in modern laser spectroscopy a time resolution has been achieved of the order of 10 fs.[5] If we analyze the behavior of the system at a time of this order after it has been "prepared," transitions may take place that would not be allowed by energy conservation. In other words, the quantum interference phenomena that produce the energy conservation are not yet complete at such short observation times.

It is clear that the classical transport theory, based on the Boltzmann equation, is not adequate for the description of the physical processes that are taking place on this time scale. In fact, semiclassical transport is based on the hypothesis, among others, that each scattering event is completed when the next one starts. For the validity of such an assumption it is necessary that the coupling between electrons and the scattering agents is sufficiently weak so that a first-order perturbation theory can be applied; this must be done in the limit of "completed collisions" so that energy conservation holds at each interaction process.

Several possible approaches have been presented for attacking the problem of quantum charge transport.[4] Serious approximations are usually necessary for obtaining manageable theoretical formulations, and very often the basic equations of the theory cannot be solved.

This situation is very similar to that in the field of nonlinear charge transport before the appearance of the Monte Carlo method that now allows the exact solution of the Boltzmann equation to be found for all physical conditions and materials. Thus it is very desirable to find an equivalent numerical method also for the case of quantum transport.

A new quantum Monte Carlo (QMC) procedure is presented here for the solution of the Liouville equation for the electronic density matrix in semiconductors. The method allows evaluation of the electronic density matrix as a function of time without any assumptions on the intensity and the duration of the electron-phonon interaction, nor on the strength of the applied field. The quantum equation is solved through a random generation of all possible quantum interactions at the various perturbative orders, in the same way as the usual classical Monte Carlo (CMC) generates classical scattering events. The principles of the method will be presented in Secs. II and III.

In the semiclassical limit (Sec. IV) our quantum treatment recovers the semiclassical Boltzmann equation, and the numerical procedure results in a new Monte Carlo procedure for the solution of semiclassical transport described by that equation.[6]

Results of the application of the present QMC method are presented in Sec. V. Section V A contains an analysis of transient transport of electrons in Si in the presence of an arbitrary high electric field, and in Sec. V B the method is applied to the problem of energy relaxation of photoexcited electrons in GaAs in the absence of electric field.

Partial accounts of this project have been presented recently.[7,8] Some numerical errors present in these preliminary data have been corrected here.

II. PHYSICAL SYSTEM AND THEORETICAL APPROACH

In order to study the properties of charge transport in a quantum scheme, let us consider an electron gas in a

semiconductor crystal, coupled to the phonon gas. Carriers are assumed to not be interacting with each other, so that the interaction of one carrier with the phonons will represent the behavior of the whole electron gas. The electron band structure is introduced in the effective-mass approximation, with a simple spherical and parabolic band.

The system is assumed to be homogeneous, and its Hamiltonian is given by

$$H = H_e + H_E + H_p + H_{e\text{-ph}} = H_0 + H_{e\text{-ph}} , \qquad (1)$$

where $H_0 = H_e + H_E + H_p$ is considered to be the unperturbed Hamiltonian since, in the effective-mass approximation, its eigenfunctions and eigenvalues are known;

$$H_e = -\frac{\hbar^2}{2m^*}\nabla^2 \qquad (2)$$

is the term corresponding to an electron in a perfect crystal (m^* is effective mass),

$$H_E = e\mathbf{E}\cdot\mathbf{r} \qquad (3)$$

describes the electric field, and

$$H_p = \sum_q \hbar\omega_q a_q^\dagger a_q \qquad (4)$$

describes the free-phonon system in the second-quantization formalism ($a_q^\dagger$ and a_q are the creation and annihilation operators of a phonon mode q). The electron-phonon interaction Hamiltonian $H_{e\text{-ph}}$ has the general form

$$H_{e\text{-ph}} = \sum_q i\hbar F(\mathbf{q})(a_q e^{i\mathbf{q}\cdot\mathbf{r}} - a_q^\dagger e^{-i\mathbf{q}\cdot\mathbf{r}}) = H_{ab} + H_{em} , \qquad (5)$$

where H_{ab} and H_{em} refer to phonon absorption and emission, respectively, and $F(\mathbf{q})$ is a function of the phonon momentum q. Its explicit form depends on the particular scattering mechanisms considered by the model. Both H_E and $H_{e\text{-ph}}$ are turned on at $t = 0$.

We have not explicitly introduced any interactions among phonons and between phonons and the thermal bath. In the numerical procedure, however, we will assume that these interactions can maintain an equilibrium phonon population during the evolution of the system.

We use the set of time-dependent basis vectors $|\mathbf{k}_0, \{n_q\}, t\rangle$ represented by

$$\frac{1}{\sqrt{V}} e^{i[\mathbf{k}(t)\cdot\mathbf{r}]} \exp\left[-i\int_0^t d\tau\,\omega(\mathbf{k}(\tau))\right]|\{n_q\}, t\rangle \qquad (6)$$

[where $\mathbf{k}(t) = \mathbf{k}_0 - e\mathbf{E}t/\hbar$ and $\omega(\mathbf{k}(t)) = \hbar k^2/2m^*$], which are the solutions of the unperturbed Hamiltonian H_0. They are direct products of electronic accelerated plane waves normalized to 1 over the crystal volume V, and the phonon states $|\{n_q\}, t\rangle$ with n_q phonons in mode q with frequency ω_q. The use of this basis is equivalent to working in the interaction representation.

The state $|\Psi\rangle$ of the system can be expanded over this set as

$$|\Psi\rangle = \sum_{\mathbf{k}_0}\sum_{\{n_q\}} c(\mathbf{k}_0, \{n_q\}, t)|\mathbf{k}_0, \{n_q\}, t\rangle . \qquad (7)$$

If we now consider the density matrix of the system in the representation of the set in Eq. (6)

$$\rho(\mathbf{k}_0\{n_q\}, \mathbf{k}_0'\{n_q'\}, t) = \langle c(\mathbf{k}_0, \{n_q\}, t)c^*(\mathbf{k}_0', \{n_q'\}, t)\rangle , \qquad (8)$$

(where $\langle\ \rangle$ is an ensemble average), the Liouville–Von Neumann equation that describes its time evolution contains only the perturbation Hamiltonian:

$$i\hbar\frac{\partial}{\partial t}\rho(X, X', t) = [H_{e\text{-ph}}(t), \rho(t)]_{X,X'} , \qquad (9)$$

where we have used the compact symbolic notation $X = (\mathbf{k}_0, \{n_q\})$.

A formal integration leads to

$$\rho(X, X', t) = \rho(X, X', 0) + \int_0^t dt_1[\mathcal{H}_{e\text{-ph}}(t_1), \rho(t_1)]_{X,X'} , \qquad (10)$$

where $\mathcal{H}_{e\text{-ph}} = (1/i\hbar)H_{e\text{-ph}}$. We are here interested in the evaluation of expectation values of electron quantities which are diagonal in the electronic part of the states in Eq. (6); thus we can focus our attention on the diagonal elements $\rho(X, t) = \rho(X, X, t)$ of ρ.

Furthermore, we will assume a diagonal initial condition for ρ decoupled in electron and phonon coordinates. This initial condition may not always correspond to a real physical situation, but it can be made plausible by assuming that the interaction is turned on at $t = 0$. The electron part is taken as some distribution function f_0 which depends on the particular problem under investigation, while the phonon part is assumed as the probability $P_{eq}(\{n_q\})$ of finding each mode q occupied by n_q phonons at equilibrium:

$$\rho(\mathbf{k}_0, \{n_q\}, 0) = f_0(\mathbf{k}_0)P_{eq}(\{n_q\}) . \qquad (11)$$

A perturbative expansion of Eq. (10) is easily obtained by iterative substitution of its right-hand side into the equation itself:

$$\rho(X, t) = \rho(X, 0) + \int_0^t dt_1[\mathcal{H}_{e\text{-ph}}(t_1), \rho(0)]_{X,X} + \int_0^t dt_1\int_0^{t_1} dt_2[\mathcal{H}_{e\text{-ph}}(t_1), [\mathcal{H}_{e\text{-ph}}(t_2), \rho(0)]]_{X,X} + \cdots$$
$$= \rho^{(0)}(X, t) + \Delta\rho^{(1)}(X, t) + \Delta\rho^{(2)}(X, t) + \cdots . \qquad (12)$$

The zeroth-order term $\rho^{(0)}(X, t)$ in the expansion (corresponding to the case of no coupling between electrons and phonons) is equal to the initial condition $\rho(X, 0)$. Since X contains the wave vectors $\mathbf{k}_0$ at $t = 0$, this contribution corresponds to the translation determined by the ballistic motion of the electrons under the sole action of the electric field without any interactions with the lattice vibrations.

The matrix element of $\mathcal{H}_{e\text{-ph}}$ between X and X' contains only the mode q related to k and k' by momentum conservation, and it is given by one of the two following expressions:

$$\mathcal{H}_{ab}(X,X',t)=F(q)e^{i\alpha(k_0,k_0',t)}e^{-i\omega_q t}$$
$$\times(n_q')^{1/2}\delta(n_q,n_q'-1)\ ,$$

$$\mathcal{H}_{em}(X,X',t)=-F(q)e^{i\alpha(k_0,k_0',t)}e^{i\omega_q t}$$
$$\times(n_q'+1)^{1/2}\delta(n_q,n_q'+1)\ ,$$
(13)

where

$$\alpha(k_0,k_0',t)=(\omega_0-\omega_0')t+\frac{e}{2m^*}(k_0'-k_0)\cdot E t^2$$

$$=[\omega(t)-\omega'(t)]t$$
$$-\frac{e}{2m^*}[k'(t)-k(t)]\cdot E t^2\ .$$
(14)

$\mathcal{H}_{ab}$ and $\mathcal{H}_{em}$ are different from zero only if the number of phonons in the mode q is changed by a unity going from X to X', since it contains only linear terms in a_q and $a_q^{\dagger}$.

The explicit form of the first-order correction is

$$\Delta\rho^{(1)}(X,t)=\int_0^t dt_1\sum_{X'}[\mathcal{H}_{e\text{-ph}}(X,X',t_1)\rho^{(0)}(X',X,0)$$
$$-\mathcal{H}_{e\text{-ph}}(X',X,t_1)$$
$$\times\rho^{(0)}(X,X',0)]\ .$$
(15)

From what we have seen regarding the matrix elements of $\mathcal{H}_{e\text{-ph}}$, it is clear that the above first-order term gives no contribution to the diagonal elements of ρ since we assumed diagonal initial conditions.

The second-order term can be rewritten, using the property

$$\mathcal{H}_{e\text{-ph}}(X,X',t)=-\mathcal{H}_{e\text{-ph}}^*(X',X,t)\ ,$$
(16)

as

$$\Delta\rho^{(2)}(X,t)=\int_0^t dt_1\int_0^{t_1}dt_2\sum_{X'}[\mathcal{H}_{e\text{-ph}}(X,X',t_1)\mathcal{H}_{e\text{-ph}}(X',X,t_2)\rho(X,0)+\mathcal{H}_{e\text{-ph}}^*(X,X',t_1)\mathcal{H}_{e\text{-ph}}^*(X',X,t_2)\rho(X,0)$$

$$+\mathcal{H}_{e\text{-ph}}^*(X,X',t_1)\mathcal{H}_{e\text{-ph}}(X,X',t_2)\rho(X',0)+\mathcal{H}_{e\text{-ph}}(X,X',t_1)\mathcal{H}_{e\text{-ph}}^*(X,X',t_2)\rho(X',0)]\ .$$
(17)

There is a simple and useful way of reading the above equation. At $t=0$ the only nonzero values of ρ are the diagonal elements; by application of $\mathcal{H}_{e\text{-ph}}$ (or $\mathcal{H}_{e\text{-ph}}^*$) the first (or the second) argument of ρ is changed from the second argument of $\mathcal{H}_{e\text{-ph}}$ to the first one; at t the two arguments of ρ are again equal (to X). Since each application of $\mathcal{H}_{e\text{-ph}}$ changes the phonon state by one unit, in order to start from a diagonal element and end up to another diagonal element, a mode q which has been absorbed (or emitted) by one argument must be absorbed (or emitted) also by the other argument or reemitted (or reabsorbed) by the same argument. Using the language of field theory, we refer to the first kind of processes as "real" emissions and absorptions, while the other ones

are referred to as "virtual processes."

Thus, taking into account the separation of $\mathcal{H}_{e\text{-ph}}$ into absorption and emission terms in Eq. (5), the contributions to be included at the second order in $\mathcal{H}_{e\text{-ph}}$ are those illustrated in Fig. 1.

With the above interpretation it is very simple to generalize the results to higher-order terms of the perturbative expansion. For example, Fig. 2 is the diagrammatic representation of one of the fourth-order contributions of the following form:

$$\mathcal{H}_{em}^*(X,X',t_1)\mathcal{H}_{ab}(X,X''',t_2)\mathcal{H}_{em}(X''',X'',t_3)$$
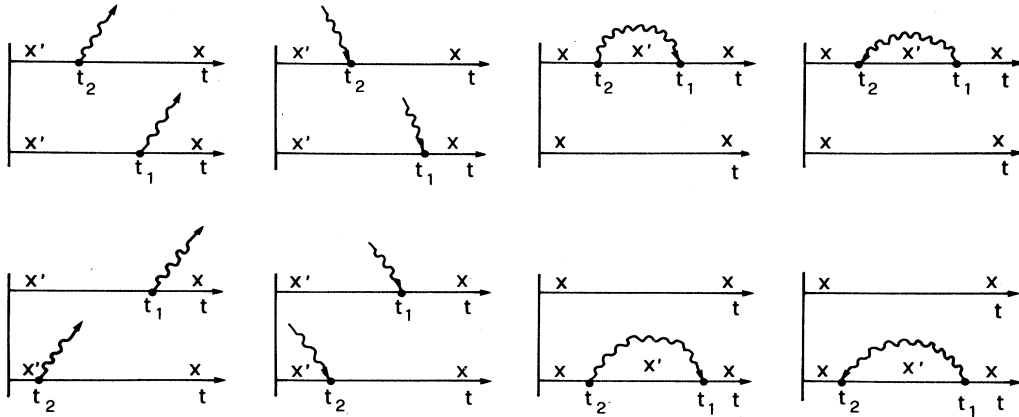$$\times\mathcal{H}_{em}(X'',X',t_4)\rho(X',0)\ .$$
(18)

FIG. 1. Diagrams representing the second-order contributions to the density matrix. The horizontal axes represent the time for the two arguments of the density matrix, and arrows indicate phonon absorption and emission processes.
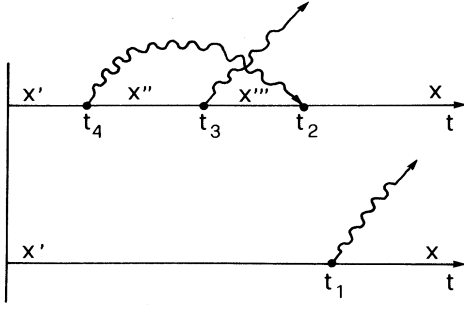
FIG. 2. Diagram representing the fourth-order contribution to the density matrix of the type shown in Eq. (18).

In this graphic representation each of the two lines represents a term in the perturbative expansion of the evolution operator of the system in the interaction representation.

Let us now recall that we start from a diagonal ρ and we are interested in the evaluation of diagonal elements of ρ. Thus the final values for the arguments of the density matrix must correspond to equal phonon states, as do their initial values. As a consequence, nonvanishing contributions come only from "paired" vertices, which correspond to complete real and virtual processes. Each process in the graphs shown in Figs. 1 and 2 corresponds to a single scattering event in classical transport.

From the analysis of these graphs of the perturbation expansion for ρ, we can focus our attention to some important aspects of the quantum description. The quantum transitions have a finite duration, during which carriers experience the action of the electric field. This effect, called the intracollisional field effect (ICFE), is obviously not present in the semiclassical description where collisions are usually considered instantaneous. Only after a certain time we obtain again a diagonal state that corresponds to a semiclassical state of the system; during the interaction the system is in a quantum state given by a superposition of $\mathbf{k}$ states which does not correspond to any semiclassical situation. Furthermore, while one process is happening, a new one can start, giving rise to multiple collisions and vertex corrections.

To recover the classical golden rule for a single scattering process it should be necessary to integrate one of the two times of the process, without interfering with other processes, over an interval large enough to obtain the Dirac δ of energy conservation in the transition probability. In addition, the effect of the field on the phase of the integrand must be neglected.

Let us now consider the reduced electronic density matrix as the trace over phonon states of the total density matrix:

$$\rho^{(e)}(\mathbf{k},\mathbf{k}',t) \equiv \sum_{\{n_{\mathbf{q}}\}} \rho(\mathbf{k},\{n_{\mathbf{q}}\},\mathbf{k}',\{n_{\mathbf{q}}\},t) \ . \tag{19}$$

The evolution equation for $\rho^{(e)}$ still contains the dynamical variables of the many-body system. In fact it is not possible to obtain a closed equation for $\rho^{(e)}$ by taking the trace of Eq. (9) for the full density matrix since the trace

operation does not commute with the interaction Hamiltonian. The reduction of the total density matrix to the electron density matrix can instead be performed in the present iterative procedure, as shown in Sec. III A.

III. NUMERICAL PROCEDURE

The numerical QMC algorithm devised for the solution of Eq. (9) is essentially based on random generations of all possible processes associated with the different perturbative corrections.

A. Fundamentals of the method

A sum $S = \sum_i x_i$ can be evaluated with the Monte Carlo technique[9] by considering the estimator x_i/p_i, where the p_i are arbitrary probabilities between zero and one normalized to unity. This estimator is then averaged over random generations of the i index selected with probabilities p_i. In fact,

$$\left\langle \frac{x_i}{p_i} \right\rangle = \sum_i p_i \frac{x_i}{p_i} = S \ . \tag{20}$$

This procedure can be easily extended to the evaluation of integrals of the type

$$\int_\Gamma f(\gamma)d\gamma \ , \tag{21}$$

where γ is the set of coordinates which describe a point in the domain Γ. In this case the estimator to be used is again $f(\gamma)/p(\gamma)$ where $p(\gamma)$ is the probability density of selecting the point γ. If $p(\gamma)$ is uniform over Γ, then

$$\int_\Gamma f(\gamma)d\gamma = V\langle f(\gamma)\rangle \ , \tag{22}$$

where the average is performed over many choices of the variable γ with uniform probability in the domain Γ, and V is the volume of this domain.

The procedures discussed above are here used to obtain an estimate of the sum in Eq. (12) that contains, in the various perturbative corrections, sums of the type described above and integrals of the general form

$$\int_0^t dt_1 \int_0^{t_1} dt_2 \cdots \int_0^{t_{n-1}} dt_n f(t_1,t_2,\ldots,t_n) \tag{23}$$

with $t > t_1 > t_2 > \cdots > t_n > 0$. In this case Eq. (22) is applicable with

$$V = \frac{t^n}{n!} \ . \tag{24}$$

The numerical procedure starts with random selections with suitable probabilities of (i) the order of the perturbative correction to be estimated; (ii) a given sequence of processes that corresponds to one of the possible contributions to the corresponding integrand; (iii) the "initial" and "final" times of the considered processes which correspond to the times at which the integrand functions are sampled; (iv) the wave vectors $\mathbf{q}$ of the phonons involved in each quantum process considered.

Then, starting from the value $\mathbf{k}(t)$ at which ρ will be evaluated, both indices of the density matrix are translated backwards in time, if we are in presence of electric

fields, down to the time of the latest vertex. At this point the matrix element $\mathcal{H}_{e\text{-ph}}$ of the interaction is evaluated, and the current value of $\mathbf{k}$ is changed accordingly. This last step of the procedure is repeated until the time of the initial condition is reached.

Due to momentum conservation of the $\mathcal{H}_{e\text{-ph}}$ matrix elements, these selections determine the argument $\mathbf{k}_{in}$ of ρ at $t=0$.

The quantity

$$\frac{\mathcal{H}_{e\text{-ph}}(t_1)\cdots\mathcal{H}_{e\text{-ph}}(t_n)}{\mathcal{P}}\rho(\mathbf{k}_{in},\{n_{q\,in}\},t=0) \qquad (25)$$

is then evaluated, where $\mathcal{P}$ is the probability of all the selections which have been made [given by the product of the probabilities of the single choices]. An average of the estimator in Eq. (25) is finally obtained through many iterations of the procedure, and it gives an estimate of ρ at time t.

In this way we obtain the density matrix through a random generation of quantum processes as we obtain the carrier distribution function and transport quantities from a random choice of carrier histories in the traditional CMC technique.

B. Phonon average

A crucial point that requires further analysis is how we perform the average over phonon variables. As we already pointed out, we assume an initial condition for ρ which is the product of an electron distribution function times the equilibrium phonon distribution; further the interaction Hamiltonian is linear in the creation and annihilation operators of modes q.

In the numerical procedure we saw that a sequence of processes is generated starting from an initial state $(\mathbf{k}_{in},\{n_{q\,in}\},0)$ which ends on the state $(\mathbf{k},\{n_q\},t)$. This sequence corresponds to a sequence of phonon wave vectors q which are absorbed or emitted on the first or on the second index of the density matrix. Since we are not interested in hot-phonon effects the electron always interacts with an equilibrium phonon bath. We can also assume that each phonon mode is chosen only once in a given sequence of processes.

If a phonon q is absorbed in a real transition and the corresponding occupation number at time t is n_q, the occupation number of the initial state must be n_q+1, and the matrix element of the interaction Hamiltonian contains the factor $(n_q+1)^{1/2}$. In order to finish the process $\mathcal{H}_{ab}$ must act on the other index of the density matrix in the same way, thus bringing the multiplicative factor n_q+1 to the numerical estimator.

In the case of virtual absorption only one index is changed from $(\mathbf{k},n_q)$ to $(\mathbf{k}'=\mathbf{k}+\mathbf{q},n_q-1)$ with an absorption, and then from $(\mathbf{k}',n_q-1)$ to $(\mathbf{k},n_q)$ at a successive time through an emission of the same phonon. The net result after the completion of the process is the presence of a multiplicative factor n_q to the numerical estimator. Analogous considerations show that for the case of real or virtual emissions the multiplicative factor is n_q or n_q+1, respectively.

At the end of the random generation we obtain for the

2n-order correction an estimator that, once averaged over the phonon states, gives to $\Delta\rho^{(e)(2n)}(\mathbf{k},t)$ the form

$$\Delta\rho^{(e)(2n)}(\mathbf{k},t)=(\text{const})\times\sum_{\{n_q\}} f_0(\mathbf{k}_{in})P_{eq}(\{n_q\}_{in})\prod_q N_q \ ,$$
$$(26)$$

where $\{n_q\}_{in}$ are the occupation numbers of the modes q in the initial state and N_q is a multiplicative factor that takes the values n_q or n_q+1, as seen above, for the phonon modes q involved into the generated sequence, and 1 for all the other phonon modes not involved in the process. Now we know that $P(\{n_q\}_{in})$ is given by the product $\prod_q P_{eq}(n_q)$.

If a phonon q is not chosen, then the sum over all possible occupation numbers n_q of $P_{eq}(n_{q\,in})$ must be equal to unity,

$$\sum_{n_q} P_{eq}(n_{q\,in})=1 \ , \qquad (27)$$

and this factor does not contribute to the product in Eq. (26).

If instead we consider a q chosen in the random generation, we have two possible cases. In the case of absorption,

$$\sum_{n_q}(n_q+1)P_{eq}(n_q+1)=n_q|_{\text{Bose}}$$

$$\text{(real absorptions)} \qquad (28)$$

$$\sum_{n_q} n_q P_{eq}(n_q)=n_q|_{\text{Bose}}$$

$$\text{(virtual absorptions)} \qquad (29)$$

where $n_q|_{\text{Bose}}$ is the equilibrium occupation number given by the Bose distribution.

In the case of emission,

$$\sum_{n_q} n_q P_{eq}(n_q-1)=n_q|_{\text{Bose}}+1$$

$$\text{(real emissions)} \qquad (30)$$

$$\sum_{n_q}(n_q+1)P_{eq}(n_q)=n_q|_{\text{Bose}}+1$$

$$\text{(virtual emissions)} \ . \qquad (31)$$

In both cases we can eventually use the Bose distribution for the evaluation of the term without introducing any approximations on the electron-phonon coupling but for the assumption that the phonon gas is constantly kept in equilibrium conditions. In full analogy with the semiclassical treatment the recipe consists in using $n_q|_{\text{Bose}}$ in the case of absorptions, and $n_q|_{\text{Bose}}+1$ in the case of emissions.

C. Improvements of the method

The QMC method described in the previous sections yields a numerical estimate of the solution of Eq. (9) through a direct generation of quantum interactions at all perturbative orders and through a numerical evaluation

of all the time integrals present in the different terms. However, the functions to be integrated are rapidly oscillating over the integration domain, owing to the quantum interference effects that they describe. Therefore in this primitive form the method would require a huge amount of computer time in order to yield a reasonably accurate result even at the lowest perturbative orders. In order to save computer time it is thus very useful to devise some methods that allow for a partial analytical evaluation of time integrals while the sum over **k** space is still evaluated through random generations of all possible terms.

The second-order perturbative correction in the interaction Hamiltonian involves only one of the processes discussed above. The explicit form of the corresponding integrals in Eq. (17) is of the type

$$\mathrm{Re} \int_0^t dt_1 \int_0^{t_1} dt_2 e^{i[2b(t_1-t_2)+a(t_1^2-t_2^2)]}$$

with

$$
\begin{aligned}
a &= \frac{e}{2m^*}(\mathbf{k}_0'-\mathbf{k}_0)\cdot\mathbf{E} \ , \\
b &= \tfrac{1}{2}(\omega_0'-\omega_0\pm\omega_q) \ ,
\end{aligned}
\tag{32}
$$

where Re stands for the real part. Here $(\mathbf{k}_0,\omega_0)$ and $(\mathbf{k}_0',\omega_0')$ refer to the interacting initial and final electron states, and ω_q is the phonon frequency. We are interested only in the real part of the integral since the diagonal elements of density matrix are real numbers. This simple expression allows a direct analytical integration in terms

are given. The result of this routine is then used for the numerical evaluation of the corresponding term.

$$\frac{\pi}{4a}\left\{\left[C\left[\frac{at+b}{\sqrt{a}}\right]-C\left[\frac{b}{\sqrt{a}}\right]\right]^2 + \left[S\left[\frac{at+b}{\sqrt{a}}\right]-S\left[\frac{b}{\sqrt{a}}\right]\right]^2\right\} . \tag{33}$$

An improvement in the efficiency of the method can be obtained also at higher orders by integrating every other vertex over the time interval determined by the times of its two adjacent vertices. The result is again expressed in terms of Fresnel integrals. Let us consider for example the case of a fourth-order correction. By recalling the following property of a double integral,

$$\int_0^t dt_1 \int_0^{t_1} dt_2 f(t_1,t_2) = \int_0^t dt_2 \int_{t_2}^t dt_1 f(t_1,t_2) \ , \tag{34}$$

we see that the application of this property to the two internal integrals present in the general expression of the term

$$\int_0^t dt_1 \int_0^{t_1} dt_2 \int_0^{t_2} dt_3 \int_0^{t_3} dt_4 f(t_1,t_2,t_3,t_4) \ , \tag{35}$$

yields

$$\int_0^t dt_1 \int_0^{t_1} dt_3 \int_{t_3}^{t_1} dt_2 \int_0^{t_3} dt_4 f(t_1,t_2,t_3,t_4) \ . \tag{36}$$

The integrals over t_4 and t_2 can now be performed analytically, each of them giving a result expressed again in terms of Fresnel integrals:

$$\mathrm{Re} \int_{t_i}^{t_j} dt' e^{i(at'^2+2bt')} = \left[\frac{\pi}{2a}\right]^{1/2}\left\{\cos\left[\frac{b^2}{a}\right]\left[C\left[\frac{at_j+b}{\sqrt{a}}\right]-C\left[\frac{at_i+b}{\sqrt{a}}\right]\right]+\sin\left[\frac{b^2}{a}\right]\left[S\left[\frac{at_j+b}{\sqrt{a}}\right]-S\left[\frac{at_i+b}{\sqrt{a}}\right]\right]\right\} . \tag{37}$$

The other two integrals cannot be performed because of the complexity of the integrand function; they must be evaluated with the numerical technique. The same procedure can be extended to higher-order corrections.

When the electric field is absent ($H_E=0$) the problems can be highly simplified because all time integrations can be performed analytically. For example, let us consider the second-order contribution due to a real emission of a phonon in mode **q** given by the first two graphs on the left in Fig. 1, which are complex conjugates of each other. The integration of these two processes yields

$$2\,\mathrm{Re} \int_0^t dt_1 \int_0^{t_1} dt_2 e^{i2b(t_1-t_2)} = \frac{1-\cos(2bt)}{(2b)^2} \ . \tag{38}$$

With similar considerations it is possible to evaluate analytically all the time integrals at all perturbative orders, even though we were not able to give a compact formula that includes all the cases (the form of each result depends in fact on the particular diagram considered). We have developed a computer routine that gives as output the symbolic primitive function of the integral, evaluated between zero and t, once the perturbative order and the details of the vertices belonging to the generated term

are given. The result of this routine is then used for the numerical evaluation of the corresponding term.

IV. SEMICLASSICAL LIMIT: BACKWARD MONTE CARLO PROCEDURE

The semiclassical limit of the theoretical approach described in the previous sections is obtained when (i) multiple collisions (crossed graphs) are neglected, (ii) ICFE is neglected, and (iii) the time between two collisions is assumed to be much longer than the collision duration, so that during each collision energy is conserved.

Under these conditions the perturbation expansion of the density matrix reduces to the analogous expansion for the distribution function obtained from the Boltzmann equation.[6]

Thus the semiclassical limit of the QMC gives a basically new CMC method for the solution of the Boltzmann equation. This new technique differs from the traditional MC method in two major respects: (1) the occurrence of particular electron histories with given scattering events is selected with arbitrary probabilities in the procedure and appropriately weighted in the estimator; (2) the elec-

tron state **k** at which the distribution function is evaluated at time t is chosen at the beginning of the procedure and electron paths are generated backward in time from t to the time $t = 0$ of the (known) initial condition. This second feature is not inherent to the method which is suitable also for a forward simulation.[11] Since the value of **k** at which f is evaluated is fixed arbitrarily, the method is particularly appealing for problems where rare regions of f are of particular interest.

V. RESULTS

This section presents numerical results obtained with the procedure discussed above for different materials and physical conditions. The analysis has been devoted to very short times after the initial conditions, when we expect quantum effects to be more evident. This choice allowed us to include perturbative corrections only up to the fourth order, which in turn limited the computer time to affordable values. Since we considered always low crystal temperatures only phonon emissions have been included, the absorption rates being negligible. Special emphasis has been given to the investigation of typical quantum effects and to the comparison with the classical case.

As an example of the computer time necessary for obtaining the results presented here we may mention that for the evaluation of the density matrix to the fourth order in a single point of **k** space about 30 CPU minutes of a Cray XMP/48 supercomputer were necessary.

A. Analysis of second- and fourth-order terms in the presence of an electric field

All the results presented in this section have been obtained starting from equilibrium conditions for the electron and phonon systems; both electric field and electron-phonon coupling are turned on at $t = 0$.

The interaction Hamiltonian of the deformation-potential interaction with optical phonons is

$$|F(q)|^2 = \frac{D^2}{2KT_{op}V\rho} . \tag{39}$$

Numerical results have been obtained for a simple-model semiconductor (relative effective mass $m^*/m_0 = 0.295$, crystal density $d = 2.33$ g/cm^3, one optical-phonon scattering with energy $T_{op} = 350$ K, and coupling constant $D = 2.5 \times 10^9$ eV cm^{-1}). The working conditions are $T = 20$ K, $E = 150$ kV/cm, $t = 50$ fs.

Figure 3 shows the quantum distribution function as a function of **k** along the field direction compared with the corresponding classical result obtained from the perturbative expansion of the Boltzmann equation (see Sec. IV). The distribution functions are peaked around the ballistic value. The particles that are scattered out of the ballistic translation are spread in a large volume of k space and cannot be seen in the figure. The quantum distribution is lower than the classical one since more particles have left their ballistic trajectories, having relaxed the requirement of energy conservation.

In order to have a better insight of the quantum effects which contribute to the result presented here it is appropriate to analyze separately the contributions of the
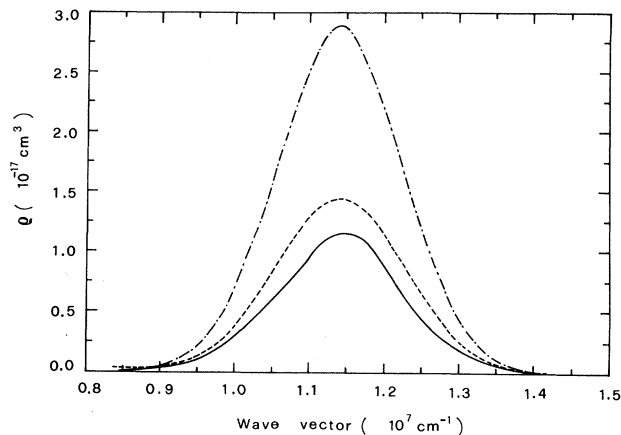
FIG. 3. Quantum electronic distribution function (solid curve) obtained from a perturbative expansion including terms up to the fourth order as a function of the electron wave vector **k** parallel to the electric field after 50 fs from the initial conditions. The result is obtained for a model semiconductor (see text). The dashed curve is the classical distribution function at the same perturbative order obtained from the Boltzmann equation. The dot-dashed curve is the initial distribution after the ballistic shift produced by the electric field.

different orders.

The second-order correction is found to be, in the region of interest, always negative due to the prevailing scattering out. Furthermore we can turn off the ICFE by neglecting the effect of the field on the phase of the matrix elements between two vertices of a particular process which would lead to the δ of energy conservation for large times; in our case, however, the completion of the transition is not necessarily reached if the time interval considered is very short.

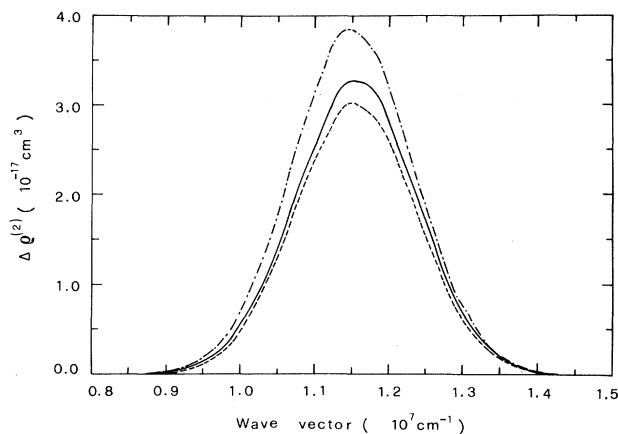In Fig. 4 we compare the absolute value of the second-

FIG. 4. Absolute value of the quantum correction (solid line) at the second perturbative order as a function of **k** parallel to the electric field compared with the absolute value of the classical one-scattering correction (dashed curve) for a model semiconductor (see text). The dot-dashed curve represents the quantum correction without ICFE.
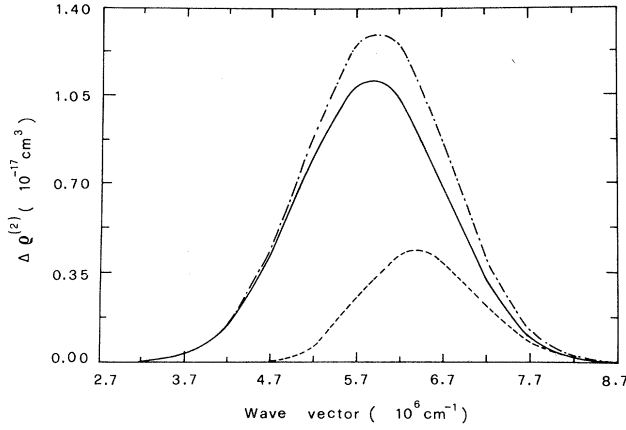
R. BRUNETTI, C. JACOBONI, AND F. ROSSI

FIG. 5. The same results as in Fig. 4 obtained for the same model semiconductor with $E = 75$ kV/cm.

FIG. 7. Quantum electronic distribution (dot-dashed curve) obtained from a perturbative expansion including terms up to the fourth order as a function of the electron wave vector **k** parallel to the electric field. The result is obtained for a simplified silicon model at $t = 0.5$ ps (see text). The solid curve is the zero-order density matrix, while the dashed curve is obtained summing terms up to the second order.

order correction as given from Eq. (17) with the same contribution without ICFE. In the same figure we also report the corresponding classical contribution that comes from "one-scattering" trajectories.[6] It can be seen that the quantum contribution is slightly larger than the classical one. However this difference is the net result of two larger quantum effects of opposite signs. In fact if the ICFE is neglected we obtain the highest curve in Fig. 4 which shows, by comparison with the classical case, the big effect of energy-nonconserving transitions, due to the short time considered. When the ICFE is also considered it reduces the scattering efficiency by reducing the time of positive interference which occurs when the energy difference between initial and final states is equal to the phonon energy.[12] It is apparent from Fig. 4 that the first effect is larger than the second since the quantum curve is higher than the classical one. This interpretation is

confirmed in Fig. 5 where the same results are shown for the case $E = 75$ kV/cm (all the other parameters are the same as in Fig. 4). Here we have reduced the ICFE through a reduction of the field strength, and the quantum result is larger than the case in Fig. 4.

Figure 6 shows the fourth-order perturbative correction (solid curve), which is now larger than zero, corresponding to two out-scattering events. We can neglect multiple collisions by allowing only processes that do not overlap, i.e., the two vertices of one given process correspond to adjacent times (dashed curve). The effect in this case appears larger than the total quantum correction.

Once the two processes have been separated, we may also neglect the ICFE in the two-scattering trajectories (dot-dashed curve). We see that the whole curve is still higher and much closer to the classical one, as it happens for the second-order term.

Finally Fig. 7 reports results for the density matrix in the case of a more realistic set of parameters that gets closer to a simplified silicon model. We changed the phonon temperature ($T_{op} = 450$ K) and the coupling constant ($D = 0.8 \times 10^9$ eV/cm). The electric field is $E = 15$ kV/cm and the time is $t = 0.5$ ps. In this case we found that the ICFE is much lower than in the previous case due to the lower field strength. Since the time is larger, the effect of multiple collisions is also lowered; we expect that this effect influences higher-order corrections.
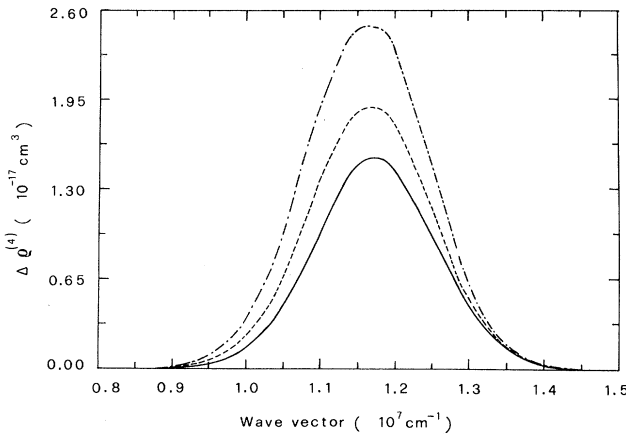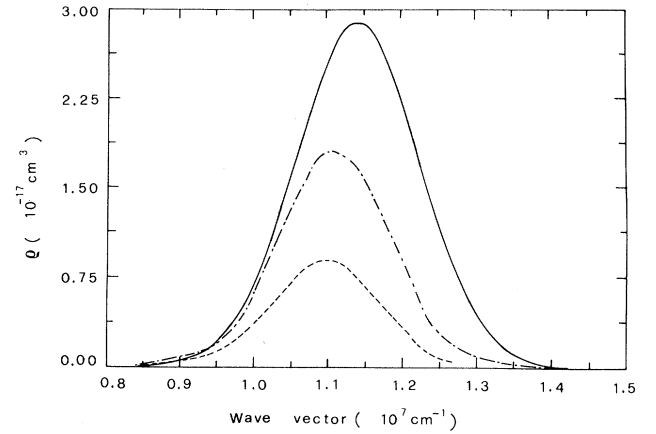

FIG. 6. Quantum corrections at the fourth perturbative order for a model semiconductor (see text). Solid curve represents the full quantum correction; dashed curve describes the quantum correction with separate collisions and the dot-dashed curve describes the quantum correction with separate collisions and without ICFE.

B. Quantum energy relaxation of photoexcited carriers in the absence of an electric field

The method described in the previous sections has been applied to the case of photoexcited electrons in bulk GaAs. The semiconductor model has been simplified to a single spherical and parabolic band similar to the one used for Si in Sec. V A. The interaction Hamiltonian in-

cludes only polar coupling to optical phonons; for such a case

$$|F(\mathbf{q})|^2 = \frac{2\pi e^2 K T_{op}}{\hbar^2 V q^2} \left[\frac{1}{\epsilon_\infty} - \frac{1}{\epsilon_0} \right] , \tag{40}$$

V is the volume of the crystal, and ϵ_∞ and ϵ_0 are the high-frequency and static dielectric constants, respectively.

Electrons are generated at $t = 0$ according to a distribution proportional to $\exp[-|\epsilon - \epsilon_0|/(KT_i)]$, where ϵ is the electron energy, and ϵ_0 and T_i are appropriate constants.

Terms up to fourth order have been included in the numerical computations. For such a reason the simulation time has been kept ≤ 100 fs. For longer times, higher perturbative orders would have been necessary. For comparison results have been obtained for the same model at the same times in semiclassical transport, using an ensemble Monte Carlo (EMC) technique.

The following parameters have been used: relative effective mass $m^*/m_0 = 0.063$, $T_{op} = 410$ K, $T = 10$ K, $T_i = 10$ K, $\epsilon_\infty = 10.92$, $\epsilon_0 = 12.9$, $\epsilon_0/K = 1000$ K.

Figure 8 shows the results obtained with EMC at $t = 100$ fs after excitation. The highest peak at 1000 K represents what is left of the initial distribution at $t = 0$. Two secondary peaks are clearly seen, corresponding to electrons having emitted one or two optical phonons. About 30% of the particles have left the original peak.

Figure 9 shows the corresponding result obtained with the present quantum Monte Carlo (note the scale change). The initial distribution is diminished of a quantity very similar to that of the classical case. However, electrons can be found, at $t = 100$ fs, in a very wide range of energies, since energy need not be conserved. The secondary peaks are not yet well formed.

If we go towards longer times the secondary peaks appear also in the quantum result, as shown in Fig. 10.

FIG. 9. Quantum electron distribution as a function of energy for a simplified GaAs model at $t = 100$ fs after excitation.

Here the time evolution of the second-order contribution to the quantum distribution function is shown up to 1 ps. It must be remembered, however, that at these long times higher perturbative orders contribute to the perturbative expansion for ρ.

Figure 11 shows the evolution in time of the electron mean kinetic energy evaluated through the density matrix shown in Fig. 9 together with the same quantity evaluated using the classical distribution function shown in Fig. 8.

From the comparison between the two curves we see that the energy relaxation in the quantum case is always weaker than the classical one at times $t \leq 100$ fs. This fact can be understood if we consider that once the requirement of energy conservation is relaxed, higher energies have a larger weight due to the larger density of states. Furthermore, due to the $1/q$ dependence of the
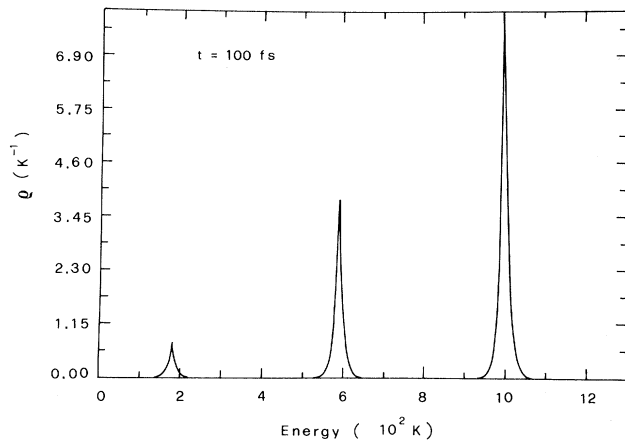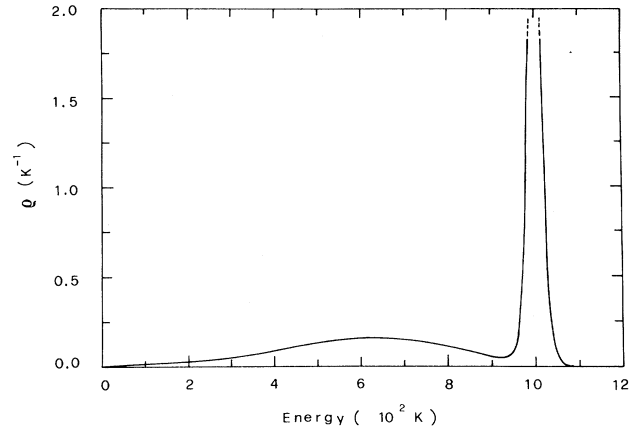

FIG. 8. Classical electron distribution as a function of energy for a simplified GaAs model at $t = 100$ fs after excitation. The highest peak at 1000 K is the initial distribution at $t = 0$.
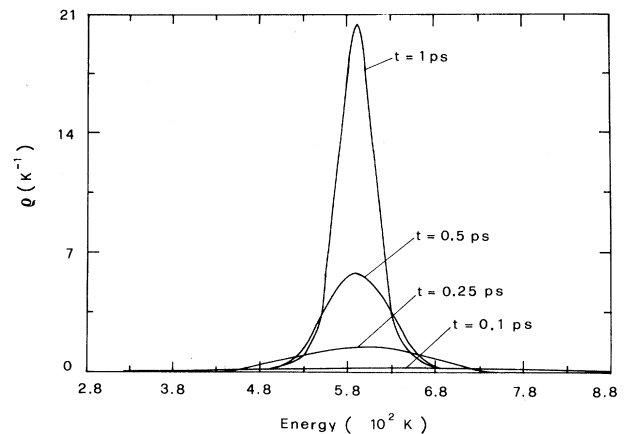

FIG. 10. Time evolution of the absolute value of the second-order contribution to the quantum distribution as a function of energy for electrons in GaAs.
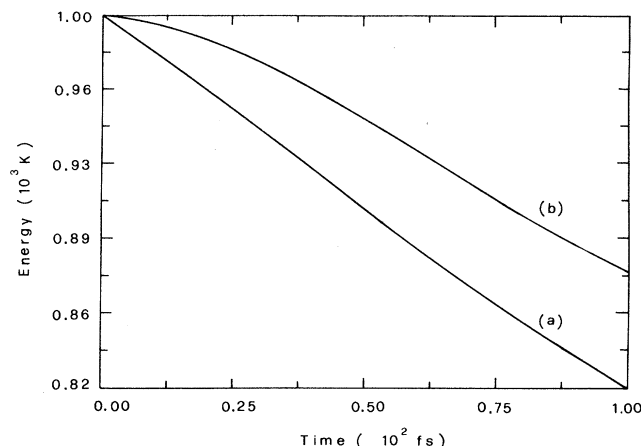
FIG. 11. Mean electron kinetic energy as a function of time, obtained with classical theory [case (a)] and quantum transport theory [case (b)] for the simplified GaAs model.

electron-phonon coupling Hamiltonian, transitions to states with energies close to the energy of the initial peak are favored.

VI. CONCLUSIONS

A quantum transport theory has been presented for transient transport of electrons in semiconductors. A theoretical approach based on the density matrix of a coupled electron-phonon system has been used, and a new numerical technique has allowed to solve the quantum equation for the diagonal part of the electron density

matrix without any assumptions about the strength of the interaction with phonons and of the applied field.

Results have been obtained at low temperatures both for Si and for GaAs using a simplified semiconductor model in both cases. For the case of Si we have analyzed the electronic density matrix up to the fourth order in the interaction Hamiltonian starting from an equilibrium carrier distribution subject to an applied electric field. For the case of GaAs we have presented the time evolution of photoexcited electrons after the excitation.

The most important effect found in every physical situation analyzed in this paper is the violation of the classical energy conservation in electronic transitions induced by phonon interaction, which appears to be dominant in the results at very short times after the initial conditions. In particular the quantum scattering at very short times appears to be more effective due to the energy-nonconserving transitions; however, energy relaxation from quantum transport has been found to be lower than what predicted by classical transport, because the same energy-nonconserving transitions favor higher energies for the final state. The weight of ICFE and multiple collisions on the quantum results have been studied and discussed.

ACKNOWLEDGMENTS

[1]C. Jacoboni and L. Reggiani, Rev. Mod. Phys. 55, 645 (1983).
[2]T. Kurosawa, J. Phys. Soc. Jpn., Suppl. 21, 424 (1966).
[3]The Physics of Submicron Structures, edited by H. L. Grubin, K. Hess, G. J. Iafrate, and D. K. Ferry (Plenum, New York, 1984).
[4]For recent reviews on the subject see L. Reggiani, Physica B+C 134B, 123 (1985); Proceedings of the International Workshop on Quantum Transport Theory with Applications to Nanometer Electronics, Italy, 1987, edited by H. L. Grubin, D. K. Ferry, and C. Jacoboni (Plenum, New York, 1988).
[5]Semiconductors Probed by Ultrafast Laser Spectroscopy, edited by R. R. Alfano (Academic, New York, 1985).
[6]C. Jacoboni, P. Poli, and L. Rota, in Proceedings of the International Conference on Hot Carriers in Semiconductors, edited

by J. Shah and G. Iafrate [Solid State Electron. 31, 523 (1988)].
[7]R. Brunetti, C. Jacoboni, P. Lugli, and L. Reggiani, in Proceedings of the 18th International Conference on The Physics of Semiconductors, edited by O. Engström (World Scientific, Singapore, 1987), p. 1527.
[8]R. Brunetti and C. Jacoboni, in Ref. 6, p. 527.
[9]J. M. Hammersley and D. C. Handscombe, Monte Carlo Methods (Methuen, London, 1964).
[10]Tables of Integrals, Series, and Products, edited by I. S. Gradshteyn and I. M. Ryzhik (Academic, New York, 1980).
[11]C. Jacoboni, P. Poli, and L. Rota (unpublished).
[12]J. R. Barker, Solid State Electron. 21, 267 (1978).